

Xylem Architecture in Giant Cacti Stems Follows Universal Scaling Theory

by

Ivanna Caspeta

A Thesis Presented in Partial Fulfillment
of the Requirements for the Degree
Master of Science

Approved April 2023 by the
Graduate Supervisory Committee:

Kevin Hultine, Co-Chair
Heather Throop, Co-Chair
Tania Hernandez

ARIZONA STATE UNIVERSITY

May 2023

ABSTRACT

Xylem conduits, a primary feature of most terrestrial plant taxa, deliver water to photosynthetic tissues and play a critical role in plant water relations and drought tolerance. Non-succulent woody taxa generally follow a universal rate of tip-to-base conduit widening such that hydraulic resistance remains constant throughout the plant stem. Giant cacti inhabit arid regions throughout the Americas and thrive in water-limited environments by complimenting water-storing succulent tissues with resource-efficient Crassulacean Acid Metabolism. Considering these adaptations, the objectives of this study were threefold: 1) determine whether xylem conduits in columnar cacti follow universal scaling theory as observed in woody taxa; 2) evaluate whether xylem hydraulic diameter is inversely correlated with xylem vessel density; and 3) determine whether xylem double-wall thickness-to-span ratio and other hydraulic architectural traits are convergent among phylogenetically diverse cactus species.

This thesis investigates the xylem anatomy of nine cactus species native to the Sonoran Desert of Arizona and Mexico, the tropical dry forests of southern Mexico, and the Alto Plano region of Argentina. Soft xylem tissues closest to the stem apex underwent a modified polyethylene glycol treatment to stabilize for sectioning with a sledge microtome. Across all species: hydraulic diameter followed a basipetal widening rate of 0.21 ($p < 0.001$), closely matching the universal rate of 0.20 for woody taxa; and xylem vessel density was inversely correlated with both length from stem apex ($p < 0.001$) and hydraulic diameter ($p < 0.001$). Double-wall thickness-to-span ratio had little to no significant correlation with either length from stem apex or hydraulic diameter. There was no significant difference in hydraulic architectural trait patterns between

phylogenetically diverse species with various stem morphologies, nor was there a significant correlation between conduit widening rates and volume-to-surface-area ratios.

This study demonstrates that giant cacti follow similar internal anatomical constraints as non-succulent woody taxa, yet stem succulence and water storage behavior in cacti remain separate from internal hydraulic architecture, allowing cacti to thrive in arid environments. Understanding how cacti cope with severe water limitations provides new insights on evolutionary constraints of stem succulents as they functionally diverged from other life forms.

DEDICATION

To my parents, my sister, and my partner, thank you for your patience, love, and encouragement throughout my graduate education. You have all been my pillar of unwavering support and without you, I would not have made it this far.

ACKNOWLEDGMENTS

I would like to personally thank my committee Co-Chair, Dr. Kevin Hultine, for welcoming me into the Dryland Plant Ecophysiology Lab and helping me find an opportunity to research cacti. Additionally, I would like to thank my other Co-Chair, Dr. Heather Throop, for providing guidance over the last couple years; and my committee member, Dr. Tania Hernandez, whose expertise is invaluable to the work presented here. I am very thankful for my outstanding committee and I appreciate your patience and wisdom throughout this journey.

Thank you to Dr. Giacomo Mozzi for introducing me to the wonderful world of cactus xylem anatomy, and for your mentorship and advice on laboratory techniques integral to this study. I am grateful to be able to collaborate with you in this study.

I would also like to thank the Desert Botanical Garden for allowing me to use the lab, resources, and cacti; as well as Dan Koepke and Ali Schuessler for kindly assisting me in the lab.

TABLE OF CONTENTS

	Page
LIST OF TABLES	vi
LIST OF FIGURES	vii
CHAPTER	
1 INTRODUCTION	1
Universal Scaling Theory in Non-Succulent Woody Taxa.....	1
Cactus Water-Use Behaviors and Water-Efficiency Strategies	4
2 METHODS	10
Collecting Xylem Tissue Samples	10
Calculating and Analyzing Conduit Architectural Traits.....	13
3 RESULTS	15
Hydraulic Diameters and Conduit Widening	15
Vessel Density	18
Double-Wall Thickness	23
Volume-to-Surface-Area Ratio	23
4 DISCUSSION	27
5 CONCLUSION	33
REFERENCES	35

LIST OF TABLES

Table		Page
1.	List of Symbols and Definitions	3
2.	List of Species, Natural Distribution, and Sampling	9

LIST OF FIGURES

Figure		Page
1.	Anatomical Features of a Radial Cactus Stem Cross-Section	5
2.	Cactus Cross-Section & Xylem Sample Diagram	11
3.	Hydraulic Conduit Diameters Widen Basipetally Across All Species	16
4.	Hydraulic Diameter: Specimen Comparison	17
5.	Vessel Density & Length from Stem Apex Across All Species	19
6.	Vessel Density & Hydraulic Diameter Across All Species	20
7.	Vessel Density for Individual Species	21
8.	Vessel Density: Specimen Comparison	22
9.	Double-Wall Thickness-to-Span Ratio & Length from Stem Apex	24
10.	Double-Wall Thickness-to-Span Ratio & Hydraulic Diameter	25
11.	Conduit Widening Rates & Volume-to-Surface-Area Ratios	26
12.	Phylogenetic Tree of Nine Cactus Species	30

INTRODUCTION

A primary feature of almost all terrestrial plant taxa is the presence of xylem conduits constructed of interconnected tubes that transport water from the rhizosphere to photosynthetic tissues. Xylem structure and function play a critical role in the overall water relations and drought tolerance of plants, as they need to deliver water to photosynthetic tissues over a wide range of biotic and abiotic conditions. Xylem conduits are located in the vascular tissue and vascular bundles throughout the plant and transport water from the roots to the photosynthetic tissues of the plant. In most vascular plants, this pathway is from the root to the leaves or the shoot tip. In cacti, xylem conduits transport water up the apex where new growth occurs as well as radially through the stem (Mauseth, 2006). Cacti inhabit arid and subtropical regions throughout the Americas and can thrive in these environments due to their unique water-use behaviors and adaptations (Williams *et al.*, 2014; Hultine *et al.*, 2019). This thesis investigates the anatomical patterns of giant cactus stem hydraulic architecture in comparison to those of non-succulent woody taxa.

Universal scaling theory in non-succulent woody taxa

In order to maintain a relatively constant hydraulic resistance over the length of the hydraulic pathway, the xylem conduits of non-succulent woody taxa generally follow a set universal rate of tip-to-base widening (West *et al.*, 1999; Anfodillo *et al.*, 2006, 2013; Olson *et al.*, 2020; Mozzi, 2021). This universal scaling theory of xylem conduit widening is described by the power law:

$$D \propto L^b \tag{1}$$

where D is the xylem conduit diameter, L is the distance from the apex, and b is the exponent that describes the rate of widening (Table 1). Following this power law, conduits widen rapidly near the stem tip and more slowly toward the base of the stem (Olson *et al.*, 2020). Previous empirical studies have established that xylem conduits widen basipetally at a universal rate of $b = 0.20$ among non-succulent woody taxa (Anfodillo *et al.*, 2013; Olson *et al.*, 2014), indicating that there are similar physical constraints on long-distance water transport in plant organs across phylogenetically diverse taxa (Anfodillo *et al.*, 2006, 2013; Olson *et al.*, 2020; Soriano *et al.*, 2020). Basipetal xylem conduit widening has developed across such taxa as an adaptation that appeals to the tradeoff between hydraulic conductivity and cavitation vulnerability (Olsen *et al.*, 2020).

Conduit widening helps woody taxa maintain a relatively constant hydraulic resistance over the length of the hydraulic pathway—in the case of plants, the height of their stems. Wider xylem conduits (or vessels) establish greater hydraulic conductivity, as described by the Hagen-Poiseuille law, which dictates that hydraulic conductivity is dependent on both conduit diameter and path length (West *et al.*, 1999). While wider xylem conduits allow for greater hydraulic conductivity, they also lose stability as size increases and become more susceptible to cavitation at a given water potential (Sperry & Tyree, 1988). Cavitation occurs when there are large bending stresses in the bordering double-walls between water-filled and air-filled, or embolized, vessels due to the negative pressure in the water-filled conduits and the resulting tension pulls air from the embolized vessels (Sperry & Tyree, 1988, Hacke *et al.* 2001, Fichot *et al.*, 2010). Thus, a balance between hydraulic conductivity and risk of cavitation is required to optimize

plant water balance under various environmental conditions. The thickness (t) and span (w) of the double-wall between conduits can influence the chances of cavitation: thicker walls relative to wall span have greater reinforcement against cavitation (Hacke *et al.* 2001). Lower thickness-to-span ratios represent weaker walls between paired conduit vessels, which can lead to decreased xylem hydraulic conductivity as xylem pressure becomes more negative due to increased incidences of embolized vessels (Fichot *et al.*, 2010; Hacke *et al.*, 2001). At the same time, to counteract the lower hydraulic conductivity of smaller vessel sizes, sapwood with smaller conduit vessels will often have a larger number of vessels (McCulloh *et al.*, 2003). In woody taxa, this increase in vessel density can be observed in the tissue near the apex of the plant stem.

Table 1. List of symbols referred to in this thesis with definitions and units.

Symbol	Definition	Units
D	Diameter	μm
L	Length from the stem apex	cm
b	Exponent of power function, rate of conduit widening	--
d	Conduit diameter	μm
D_h	Hydraulic mean diameter	μm
V	Stem volume	m^3
S	Stem surface area	m^2
t	Conduit double-wall thickness	μm
w	Conduit double-wall span	μm

Basipetal widening has been extensively researched throughout a wide selection of phylogenetically diverse non-succulent woody taxa (Anfodillo *et al.*, 2006; 2013; Olson *et al.*, 2014; 2020; Soriano *et al.* 2020), but it has only begun to be explored in cacti (Mozzi, 2021; Caspeta, 2022).

Cactus water-use behaviors and water-efficiency strategies

Cacti inhabit arid and subtropical regions throughout the Americas and can thrive in these stressful, water-limited environments by complimenting the water-storage capacities of their succulent parenchymatous tissue with resource-efficient Crassulacean Acid Metabolism (CAM; Nobel, 1991; Nobel, 1996; Williams *et al.*, 2014; Hultine *et al.*, 2019; Mozzi 2021). Almost a third of cactus species are among the most threatened taxa and will likely remain under threat as the impacts of climate change continue (Hultine *et al.*, 2023). Within the family Cactaceae, giant columnar cacti in particular hold important cultural, economic, and ecological value throughout the regions they inhabit (Williams *et al.*, 2014; Hultine *et al.*, 2016). Columnar cacti as described in this thesis are those of gigantic growth forms with ribbed stems and can be single- or multi-stemmed (Mauseth, 2006).

One important adaptation that sets giant cacti apart from other vascular plants is the succulent parenchymatous tissue located between the dermis layers and the vascular system that store massive amounts of water that helps these plants survive droughts (Mauseth, 2000; Mauseth, 2006). Figure 1 displays half of a radial cross-section of a de-spined cactus stem and its anatomical features. The dermis layers of the plant include the epidermis that facilitates gas exchange and the thick hypodermis that provides rigidity and strength to support the expansion of the cortex (Mauseth, 2006). The cortex is the

main organ that cacti use to store excess water. The outer cortex, located within the ribs of the stem, contains both chlorophyllous and water-storage tissue, while the inner cortex located between the base of the ribs and the central vascular system is primarily used for water storage (Mauseth, 2006). Xylem tissue can be found in the woody vascular tissue in the cactus stem, between the cortex and the pith. The pith can store both water and starches and helps facilitate the radial movement of water from the center of the stem out into the photosynthetic tissues in the outermost cortex (Mauseth, 2006).

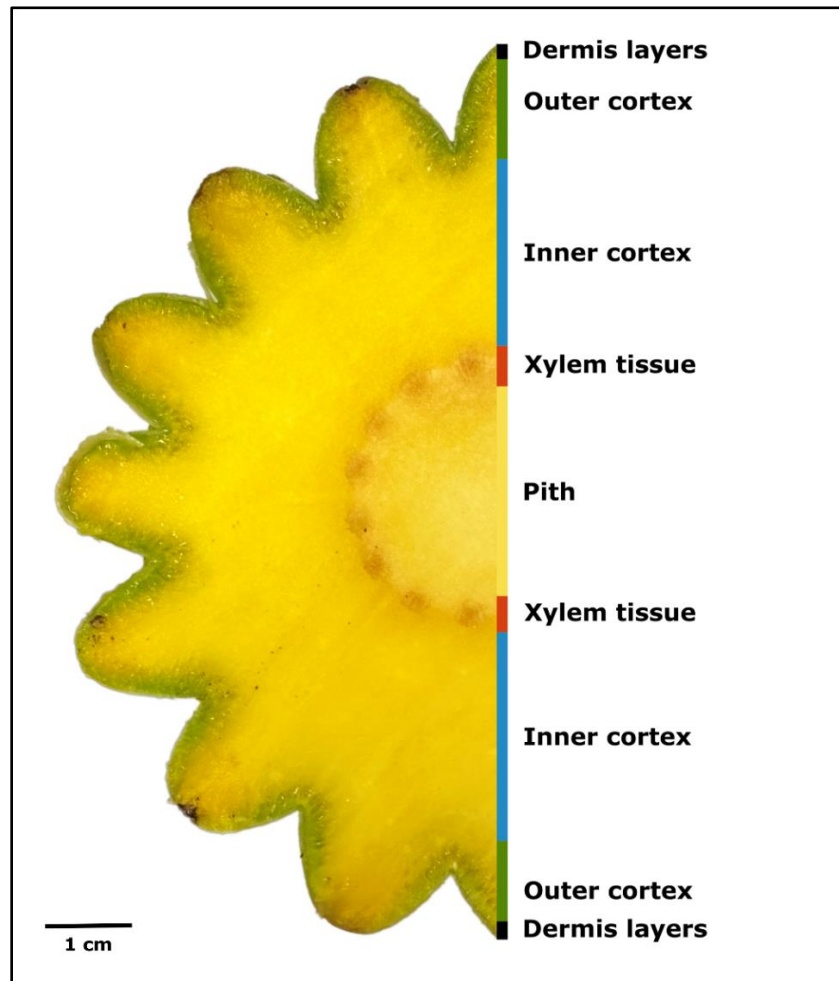


Figure 1. Anatomical features of a radial cross section of a de-spined cactus stem: dermis layers, outer and inner cortex, xylem (vascular) tissue, and pith.

The succulent water-storage tissue in cactus stems decouples water transport into the stem from gas exchange and allowing the plant to function as usual regardless of whether soil water is available (Mozzi 2021). The primary driver of long-distance water transport in cacti is therefore not stomatal regulation of water vapor to the surrounding atmosphere, but rather osmotic gradients in their stem storage tissues.

Cacti are also a part of the 6% of angiosperm species that utilize CAM photosynthesis as opposed to the largely dominant C3 photosynthetic pathway, and as a result are able to avoid excessive evapotranspiration (Silvera *et al.*, 2010; Bräutigam *et al.*, 2017). CAM photosynthesis temporally separates the photosynthetic reactions between day and night. At nighttime when evapotranspiration rates are low, CAM plants open their stomata to acquire carbon dioxide to assimilate into a 4-carbon sugar called malate. During the daytime, the stomata of CAM plants close to avoid high evapotranspiration rates. Concurrently, malate is decarboxylated back into carbon dioxide and the Rubisco enzyme is exposed to a higher concentration of carbon dioxide than occurs in C3 plants (Winter *et al.*, 2005; Berry *et al.*, 2013). Consequently, the water use efficiency—the ratio of carbon dioxide fixation to loss of water—of CAM plants is far greater than that of C3 plants. CAM plants require less water for an equal accumulation of biomass than C3 plants when grown in similar conditions, making them well-adapted to arid environments (Nobel, 1991; Winter *et al.*, 2005).

Cacti display various growth forms and water-use strategies. Even within columnar cacti, water storage behaviors can vary greatly. Volume-to-surface-area (V:S) ratios well represents such variation between columnar cactus species. The V:S ratio of a given cactus stem reflects physiological trade-offs between the water storage capacity of

succulent tissues and whole-stem photosynthetic capacity (Williams *et al.*, 2014). Columnar cactus species with lower V:S ratios have a greater photosynthetic capacity, which can be beneficial for growth and reproduction under favorable environmental conditions. Conversely, species with higher V:S ratios have a greater water storage capacity, which can be beneficial during droughts (Williams *et al.*, 2014; Hultine *et al.*, 2019). Such tradeoffs could influence xylem conduit patterns in columnar cacti.

Investigating xylem architecture in giant columnar cacti

Despite their divergent morphologies, cacti share a similar vascular system to woody taxa that is composed of vascular bundles that comprise both xylem and phloem tissues (Mauseth, 2006). Thus, it remains an open question whether xylem architecture of cacti follows similar conduit scaling laws as non-succulent plant taxa. The objectives of this study were threefold. 1) Determine whether columnar cacti follow the same “universal” rate of apex-to-base xylem widening observed in woody plant taxa. 2) Evaluate whether xylem hydraulic mean diameter is inversely correlated with xylem vessel density. And 3) investigate whether hydraulic architecture, including the previously mentioned hydraulic diameter and vessel density, as well as conduit double-wall thickness-to-span ratio, is convergent among phylogenetically diverse cactus species.

We studied the xylem anatomy of nine phylogenetically diverse giant arborescent and columnar cactus species (Table 2) native to the Sonoran Desert of Arizona and Mexico, the tropical dry forests of southern Mexico, and the Alto Plano region of Argentina. We investigated mean hydraulic diameter, vessel density and conduit double-wall thickness-to-span ratio measured at multiple distances on the stems (n = 1 to 6 stems

per species) of several young specimens of these species, all under 2 m tall. I predicted that given the adaptations of cacti that allow them to thrive in arid environments and reduce the stress of water loss and lack of available external water: a) cacti will follow a basipetal conduit widening pattern similar to the universal pattern previously reported in non-succulent woody plant taxa; b) to compensate for smaller vessel diameters near the stem apex, vessel density will be higher near the stem apex than at the base; and c) the double-wall thickness-to-span ratio of paired conduit vessels and other hydraulic architecture will be similar among cactus species despite their different morphologies and phylogenetic diversity.

Table 2. List of species, natural distribution range, stem height, and number of cross-sections per stem. Multiple stem heights and section numbers reported indicate multiple stems sampled. Stems listed are either newly acquired, *from Caspeta (2022), or **from Mozzi (2021).

Species	Natural distribution range	Stem height (cm)	Number of sections
<i>Carnegiea gigantea</i>	Mexico and USA	55**	6
		50**	6
		44*	3
		40**	4
		35*	2
		29*	4
<i>Echinopsis spachiana</i>	Argentina and Bolivia	65**	5
<i>Echinopsis terscheckii</i>	Argentina and Bolivia	87**	13
<i>Neobuxbaumia tetetzo</i>	Mexico	55**	6
<i>Pachycereus pringlei</i>	Mexico	63**	6
		55**	5
<i>Pachycereus weberi</i>	Mexico	85**	6
<i>Lophocereus schottii</i>	Mexico and USA	55**	6
<i>Stetsonia coryne</i>	Argentina, Bolivia and Paraguay	70**	6
<i>Stenocereus thurberi</i>	Mexico and USA	180	6
		175	7
		170	6
		90**	9
		79*	6
		70**	6

METHODS

Collecting xylem tissue samples

This study compiled data on young specimens under 2 m tall of nine giant columnar cacti species with columnar and arborescent adult growth forms from Mozzi (2021) with data on *Carnegiea gigantea* and *Stenocereus thurberi* from Caspeta (2022) and additional xylem conduit data obtained from *S. thurberi* specimens grown outdoors and collected from the Desert Botanical Garden (DBG) in Phoenix, AZ. Existing cactus xylem data from Mozzi (2021) and Caspeta (2022) was similarly acquired from cactus stems grown outdoors under uniform conditions. Table 2 displays the list of all species included in the study, their natural range of distribution, total length from base to apex of each stem sampled, and total number of cross-sections per stem.

Newly acquired cactus specimens were processed at the Dryland Plant Ecophysiology Lab at the DBG. Each stem was de-spined with small clippers and pliers to avoid injury during stem dissection and sampling. Stems were then cross-sectioned at multiple lengths from the stem apex depending on the total height of the stem (new data: $n = 6$ to 7 cross-sections per stem, existing data: $n = 2$ to 13). Cross-section sampling was concentrated near the stem apex to better capture the non-constant variation of hydraulic architecture as reported in non-succulent woody taxa, where xylem conduits widen quickly within a short distance from the apex of the stem. Each stem cross-section was photographed with a 1 cm piece of paper for accurate scaling during cross-section surface area (cm^2) and total xylem tissue area (cm^2) measurements (Figure 2A).

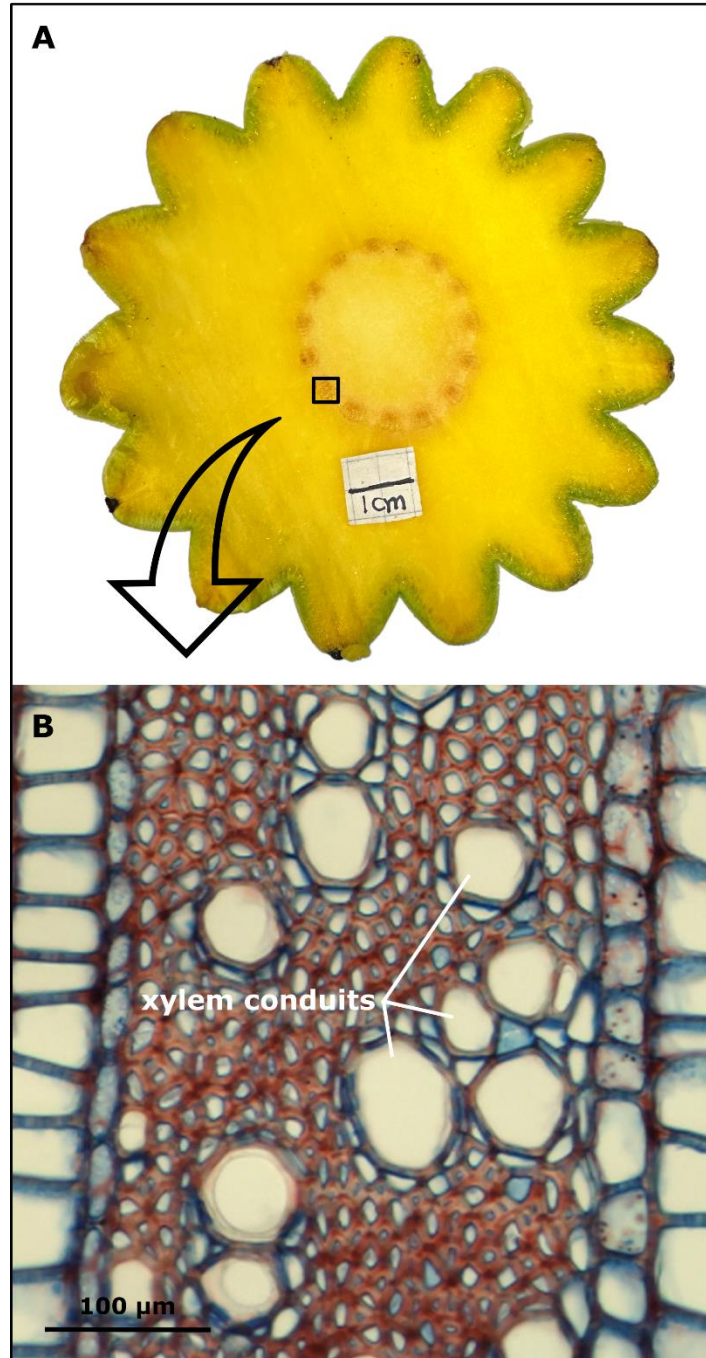


Figure 2. Cactus samples taken 80 cm from the apex from a *Stenocereus thurberi* specimen. **A:** Radial cross-section of a de-spined stem; xylem tissue outlined in black provides an example of where samples were isolated from the cross-section. **B:** Double-stained xylem tissue sample with identification of xylem conduits.

From each stem cross section, 3-4 samples of xylem tissue were isolated from the side corresponding to the selected length from stem apex. Careful attention was taken to avoid sampling uneven xylem tissue that can occur when stems grow at an angle. Each sample of xylem tissue was sectioned with a GSL1 sledge microtome equipped with A-type 0.38 NT-cutter paper-knife blades. The blades were replaced at each new stem cross-section to maintain sufficient sharpness for creating xylem tissue slices 20 μm in width. Each xylem tissue sample was carefully sliced and placed from the microtome blade to a microscope slide using a small brush. During the sampling process, the xylem tissue samples and slices were kept hydrated with deionized (DI) water.

To differentiate between lignified and non-lignified cells, the xylem tissue slices were double-stained (Figure 2B) by adding 5-6 drops of 1:1 mixture of safranin and astra blue dyes to the samples on microscope slides. The xylem tissue slices were soaked in the dye mixture for 10 minutes, then rinsed with DI water to avoid staining diffusion and flushed with consecutive solutions of 50%, 70%, and 100% ethanol to remove moisture. After dehydration, the xylem tissue slices were dried with lint-free paper towels and permanently mounted onto the microscope slides using Permount mounting medium. Completed microscope slides were set to dry between magnets for at least 24 hours.

Xylem tissue samples within 10 cm of the stem apex underwent a modified polyethylene glycol (PEG) treatment to stabilize soft xylem tissues for microtome sectioning, following the procedure outlined in *Mozzi et al. (2021)*. This procedure involves: 1) submerging each sample of xylem tissue taken from cross-sections within 10 cm from the apex in a 25% solution of PEG in DI water, covering the solution to avoid evaporation of water, and leaving it for 24 hours; 2) transferring the xylem samples to a

50% PEG solution, covering again and leaving it for another 24 hours; and 3) transferring the samples to a 70% PEG solution and baking them at 60°C until all water evaporated. After infiltration with PEG, the xylem tissue samples were sectioned as usual with the sledge microtome, with the exception of using ethanol instead of water to prevent the xylem tissue from drying out before staining, as PEG is water soluble.

Completed and dried microscope slides were photographed at 10x magnification with a Moticam Pro 282A camera mounted on an Olympus CX41 light microscope. Xylem tissue and stem cross section photographs were measured with ImageJ (ImageJ 1.53k) and scaled using a calibration of 0.15 mm and 1 cm, respectively.

Calculating and analyzing conduit architectural traits

Xylem conduit diameters (d) were calculated as the diameter of an equivalent circle from vessel area measurements of at least 100 xylem vessels per length from stem apex. Hydraulic mean diameter (D_h) was then calculated at each length according to the following equation from Anfodillo *et al.* (2006) and Mozzi (2021),

$$D_h = \frac{\sum_{n=1}^N d_n^5}{\sum_{n=1}^N d_n^4} \quad (2)$$

This equation reflects the actual conductance of various-sized xylem conduits as it considers the disproportionate contribution of larger conduits to hydraulic conductivity, given that a few large conduits can transport the same amount of water as many small ones (Sperry *et al.* 1994). Xylem vessel density was calculated as vessels/mm², measuring the vessel count over xylem tissue area and averaged for each length from stem apex.

Double-wall thickness-to-span ratio was measured as $(t/w)_h^2$, where wall span (w) is the length of the border between the paired vessels and double-wall thickness (t) is the

average thickness at three points—at each end and at the midpoint—along the border where vessels are joined. $(t/w)_h^2$ was measured in *S. thurberi* and *C. gigantea* and calculated from measurements of paired vessels where at least one vessel is within +/- 8 μm (Fichot *et al.*, 2010) of the hydraulic mean diameter at that length from stem apex (n = 1 to 26).

Volume-to-surface-area ratios (V:S, $\text{m}^3 \text{m}^{-2}$) were calculated as the ratio of cross-sectional area to perimeter from cross-section images. Cross-sectional area and perimeter accurately represent volume and surface area, respectively, since in columnar ribbed cacti both of the former can be multiplied by the total stem length to get the latter (Mauseth, 2000; Williams *et al.*, 2014). V:S ratios were calculated at each cross-section and then averaged per species.

All data were analyzed using R (R Core Team, 2020), RStudio (Posit team, 2022), and the tidyverse package (Wickham, 2017). Hydraulic diameter, vessel density, and double-wall thickness-to-span ratio were tested for normality in R using the Shapiro-Wilk test and each species was tested against each other using an ANOVA and Tukey test. Using the tidyverse package, a logarithmic regression analysis was performed on hydraulic diameter and vessel density data to calculate the rate of conduit widening and rate of vessel density change, respectively. This was done for all species in total and individually. Double-wall thickness-to-span ratio and V:S ratio underwent a linear regression analysis. For all tests, only P values of less than 0.05 were considered significant.

RESULTS

Hydraulic diameters and conduit widening

Hydraulic diameters (D_h , μm) widened at a rate of 0.211 ($R^2 = 0.613$, $p < 0.001$) when plotted against length from stem apex (cm) for all nine columnar cactus species (Figure 3A), which is nearly identical to the theoretical rate of widening of 0.20 (Olson *et al.*, 2020). When plotted for each individual species (Figure 3B), the rate of widening (b) ranged from 0.113 in *Echinopsis spachiana* ($R^2 = 0.871$, $p = 0.020$) to 0.361 in *Pachycereus weberi* ($R^2 = 0.896$, $p = 0.001$). All individual species widening rates were significant ($p < 0.050$) and 7 out of 9 species had strong correlation between hydraulic diameter and length from stem apex ($R^2 > 0.700$). *C. gigantea* and *Pachycereus pringlei* had slightly lower correlation with length from stem apex ($R^2 = 0.573$ and $R^2 = 0.602$, respectively). However, there was no significant difference in conduit widening rates between the individual species.

Figure 4 shows the hydraulic diameters for individual *C. gigantea* and *S. thurberi* specimens. The conduit widening rates in *S. thurberi* ranged from 0.120 to 0.198 ($p < 0.050$), while in *C. gigantea* they ranged from 0.239 to 0.305 ($p < 0.050$). While there was slight variation, there was also no significant difference in conduit widening rates between different specimens of the same species.

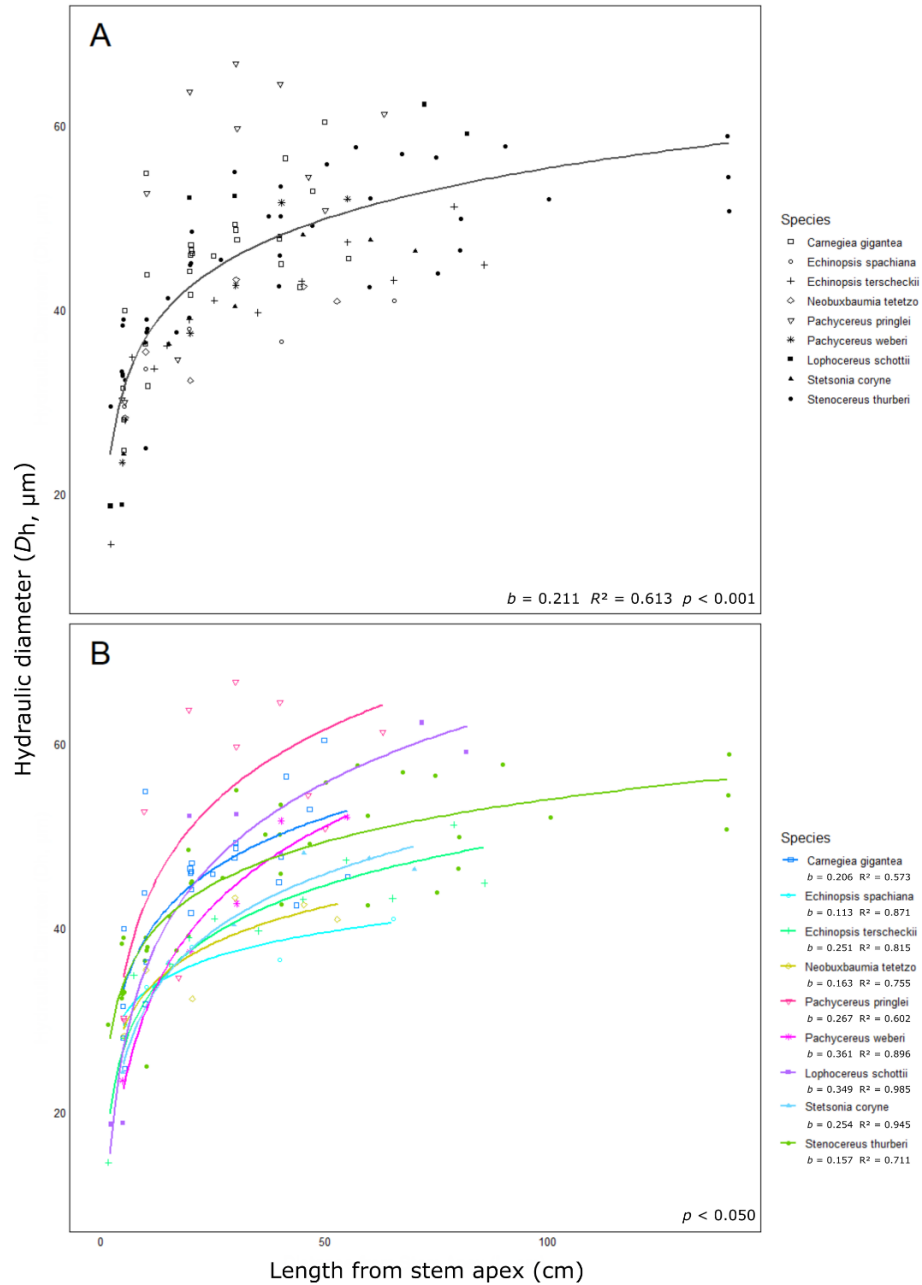


Figure 3. Hydraulic diameters (D_h , μm) along the length from the stem apex (cm) in all specimens across nine columnar cactus species ($n = 20$ stems). **A:** Conduit widening rate of all species, differentiated by shape, was 0.211 ($R^2 = 0.613$, $p < 0.001$). **B:** Conduit widening rates for each species, differentiated by color and shape, ranged from 0.113 in *E. spachiana* ($R^2 = 0.871$, $p = 0.020$) to 0.361 in *P. weberi* ($R^2 = 0.896$, $p = 0.001$).

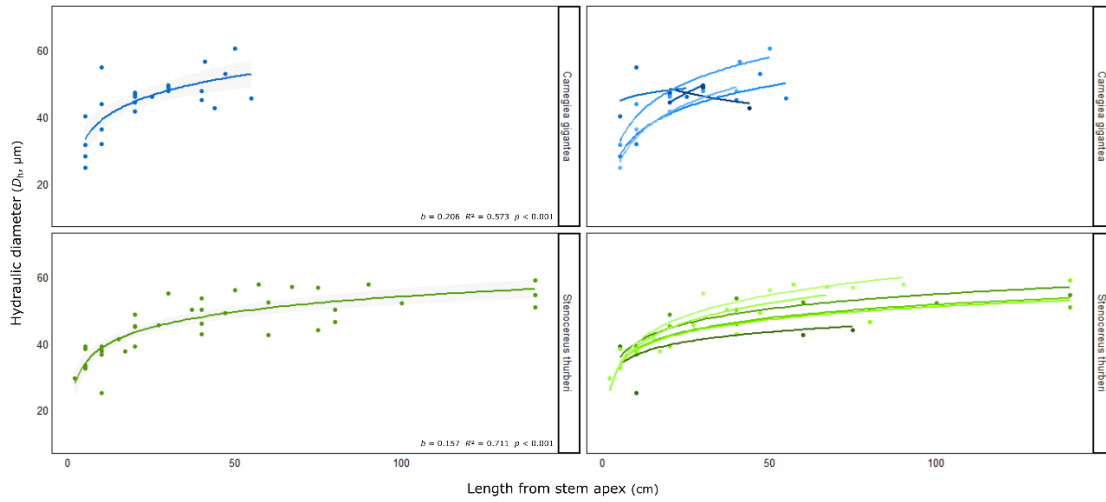


Figure 4. Hydraulic diameters (D_h , μm) along the length from the stem apex (cm) for *C. gigantea* (blue) and *S. thurberi* (green). Graphs on the left show the logarithmic curve for each species, while graphs on the right show logarithmic curves for each stem specimen sampled ($n = 6$ per species). Conduit widening rates for *S. thurberi* specimens ranged from 0.120 to 0.198 and for *C. gigantea* specimens from 0.239 to 0.305 ($p < 0.050$).

Vessel density

Across all species, vessel density (vessels/mm²) decreased at an exponential rate of -0.701 ($R^2 = 0.715$, $p < 0.001$) when plotted against length from stem apex and fitted with a logarithmic regression line (Figure 5). Additionally, there was a significant inverse correlation between vessel density and hydraulic diameters across all species that followed an exponential rate of -2.804 (Figure 6, $R^2 = 0.751$, $p < 0.001$).

Individual species showed significant exponential decrease in vessel density along length from the stem apex (Figure 7), with exponential rates ranging from -1.174 in *Neobuxbaumia tetetzo* ($R^2 = 0.821$, $p = 0.013$) to -0.358 in *E. spachiana* ($R^2 = 0.904$, $p = 0.013$). Vessel density trends had a strong correlation with distance from the stem apex ($R^2 > 0.800$) and decreased significantly ($p < 0.050$) for all individual species. However, there was no significant difference in vessel density trends between individual species.

Figure 8 shows the exponential decrease in vessel density for individual *C. gigantea* and *S. thurberi* specimens. Significant exponential rates of vessel density ranged from -0.892 to -0.446 in *S. thurberi*, and from a slope of -1.215 to -0.490 in *C. gigantea* ($p < 0.050$). While there was slight variation, there was again no significant difference in the exponential trends between different specimens of the same species.

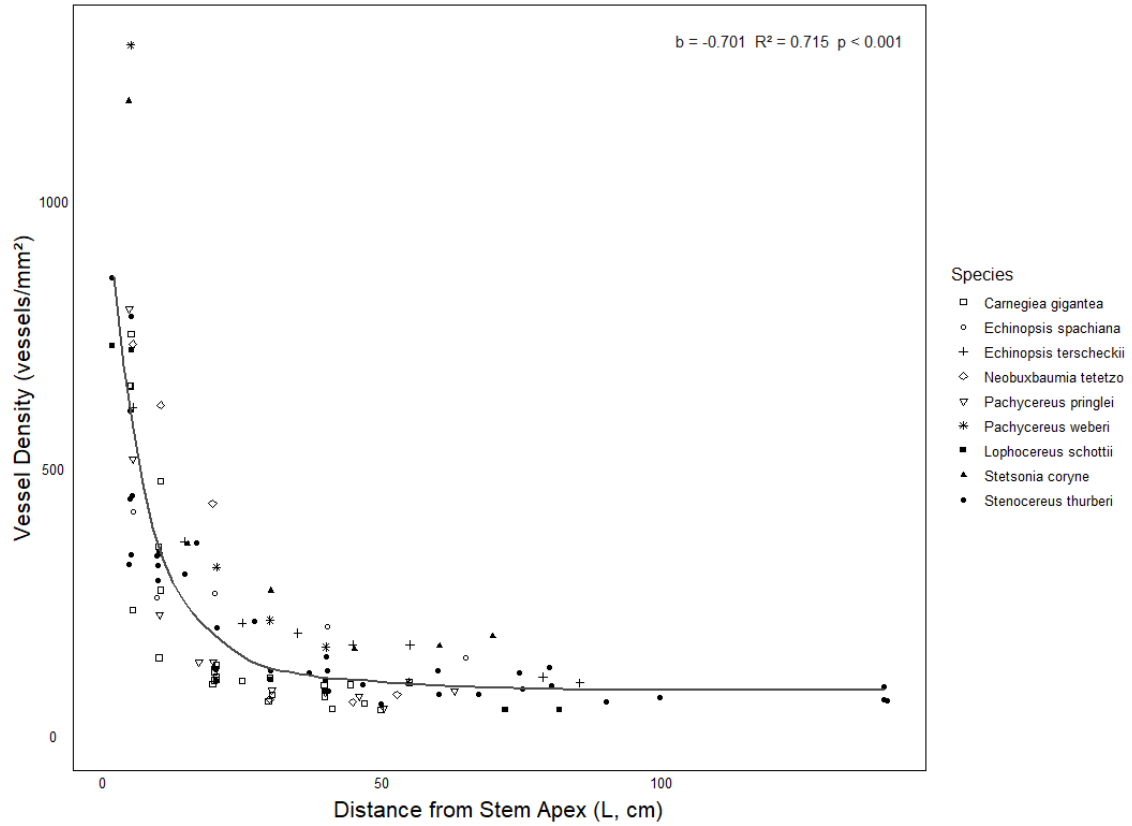


Figure 5. Vessel density (vessels/mm²) along the length from the stem apex (cm) across all species, differentiated by shape, decreased at an exponential rate of -0.701 ($R^2 = 0.715$, $p < 0.001$).

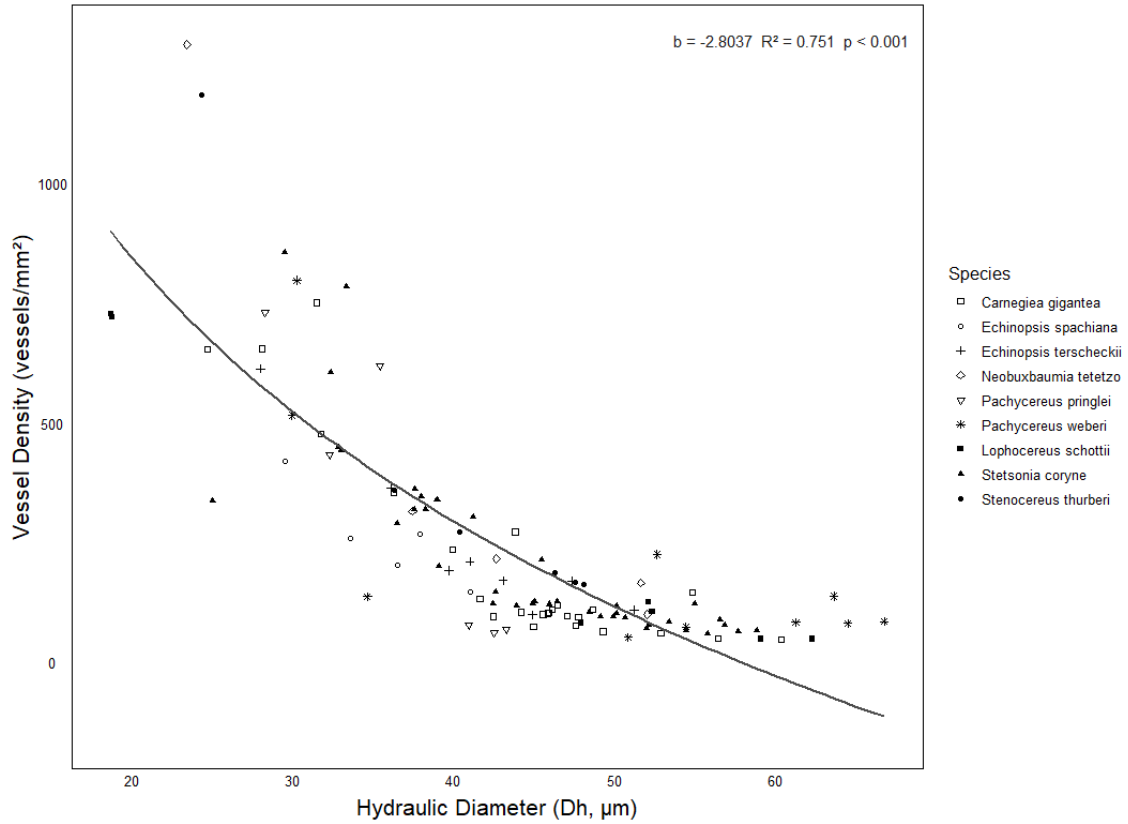


Figure 6. Vessel density (vessels/mm²) in relation to hydraulic diameter (D_h , µm) across all species, differentiated by shape. Vessel density decreased with hydraulic diameter at an exponential rate of -2.804 ($R^2 = 0.751$, $p < 0.001$).

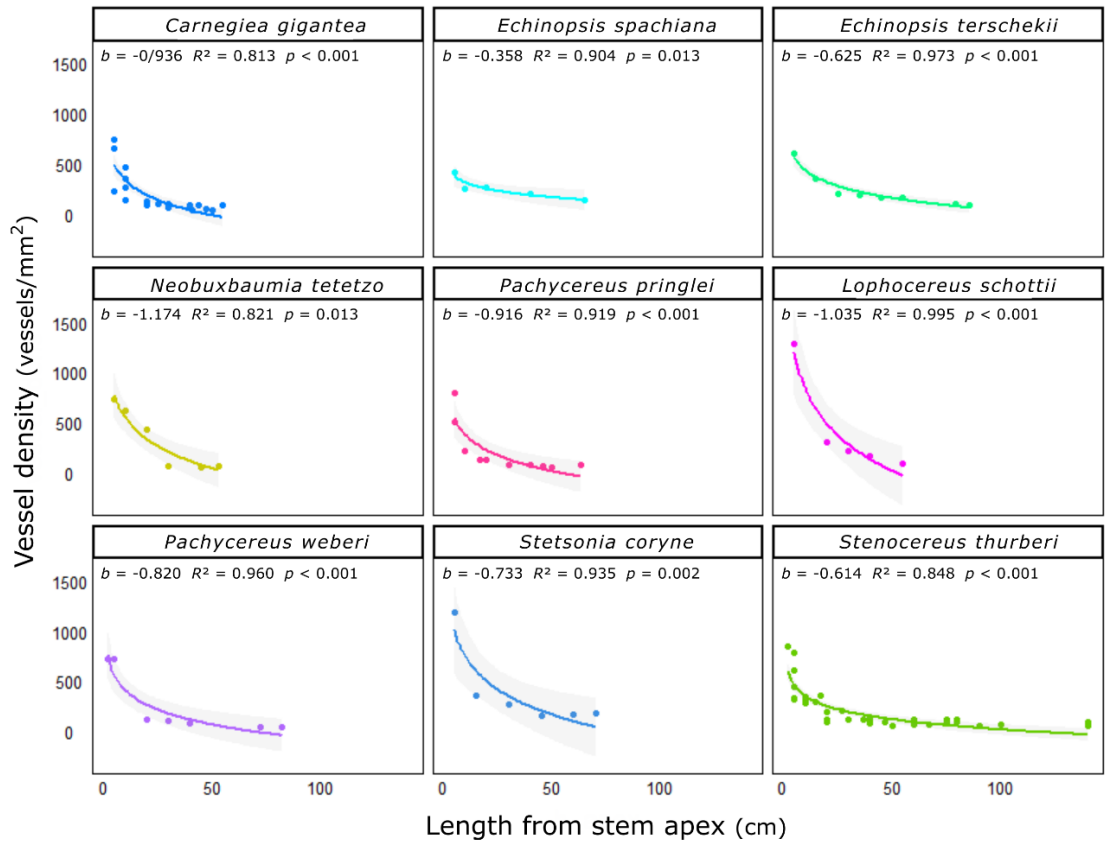


Figure 7. Vessel density (vessels/mm²) along the length from the stem apex for each of nine columnar cactus species. Rates of decreases in vessel density ranged from -1.174 in *N. tetetzo* ($R^2 = 0.821$, $p = 0.013$) -0.358 in *E. spachiana* ($R^2 = 0.904$, $p = 0.013$).

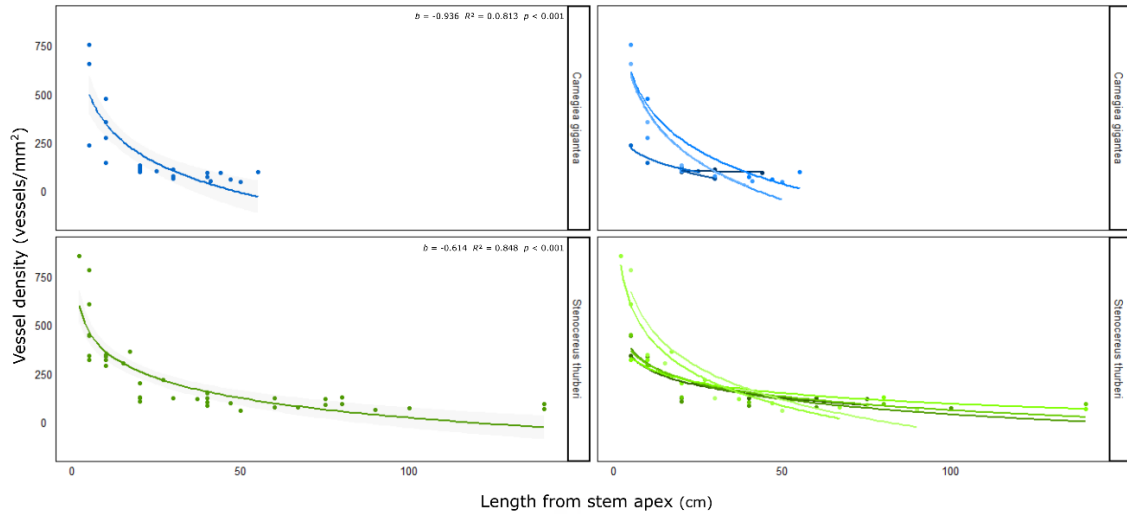


Figure 8. Vessel density (vessels/mm²) along the length from the stem apex for *C. gigantea* (blue) and *S. thurberi* (green). Graphs on the left show the logarithmic curve for each species, while graphs on the right show logarithmic curves for each stem specimen sampled (n = 6 per species). Vessel density decreased at exponential rates ranging from -0.892 to -0.446 in *S. thurberi* and from -1.215 to -0.490 in *C. gigantea* ($p < 0.050$).

Double-wall thickness

In *C. gigantea* and *S. thurberi* specimens, double-wall thickness-to-span ratio, $(t/w)_h^2$, decreased at a rate of -0.001 in both species when plotted against length from stem apex (Figure 9). However, the linear model was only significant for *S. thurberi*, although the model did not fit the data well ($R^2 = 0.024$, $p = 0.005$). The trendline for *C. gigantea*, despite having a similar rate of decrease, showed no significant correlation with length from stem apex ($R^2 = 0.012$, $p = 0.467$).

When $(t/w)_h^2$ was plotted against hydraulic diameter (Figure 10), each species showed a different rate of change, and again only the linear model for *S. thurberi* was significant but did not fit well ($b = -0.059$, $R^2 = 0.040$, $p < 0.001$). The linear model for *C. gigantea* showed no significant correlation ($b = -0.012$, $R^2 = 0.001$, $p = 0.861$). Double-wall thickness (t , μm) increased significantly with hydraulic diameter at a rate of 0.059 in *S. thurberi*, although the linear model did not fit well ($R^2 = 0.040$, $p < 0.001$). In *C. gigantea*, there was no significant change with hydraulic diameter ($R^2 = 0.001$, $p = 0.861$).

Volume-to-surface-area ratio

Across all species, when comparing the conduit widening rate (b) to volume-to-surface-area (V:S) ratio (m^3m^{-2}), there was no significant correlation ($R^2 = 0.011$, $p = 0.787$). Figure 11 shows the conduit widening rate and V:S ratio for each of the nine species.

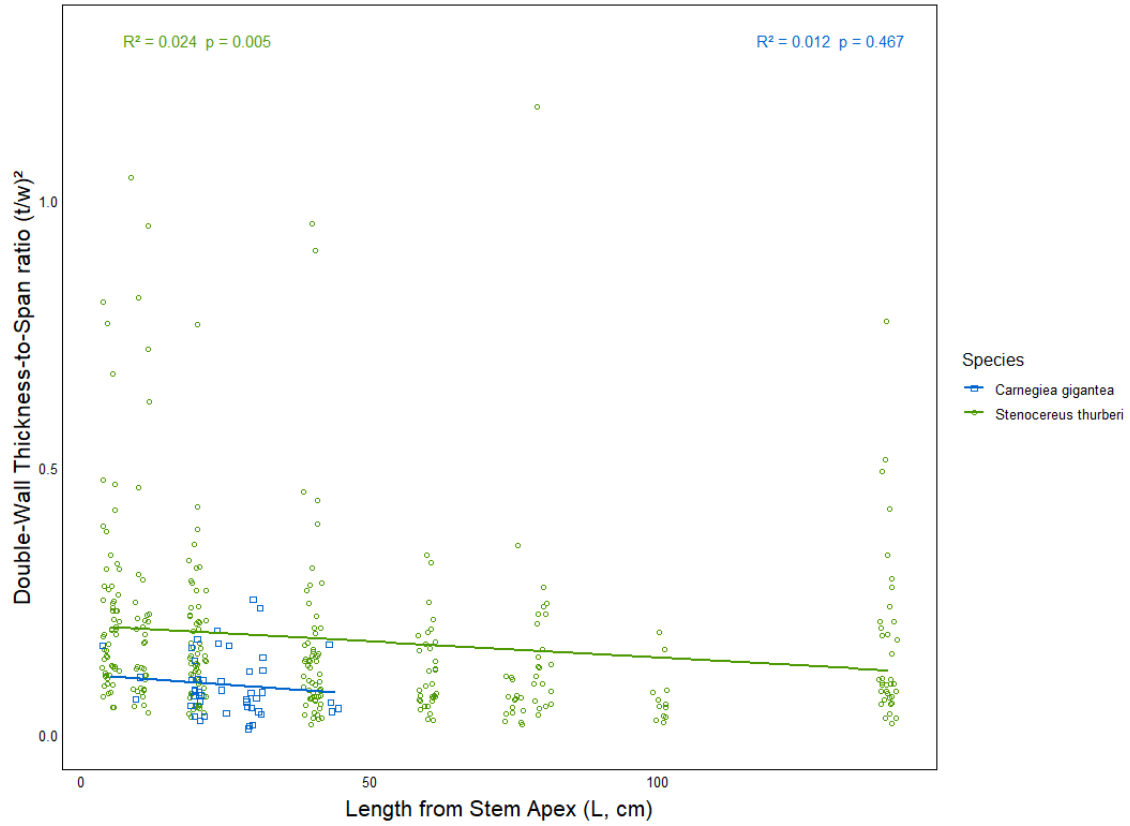


Figure 9. Double-wall thickness-to-span ratio $(t/w)_h^2$ over length from stem apex (cm) in *C. gigantea* ($b = -0.001$, $R^2 = 0.012$, $p = 0.467$) and *S. thurberi* ($b = -0.001$, $R^2 = 0.024$, $p = 0.005$).

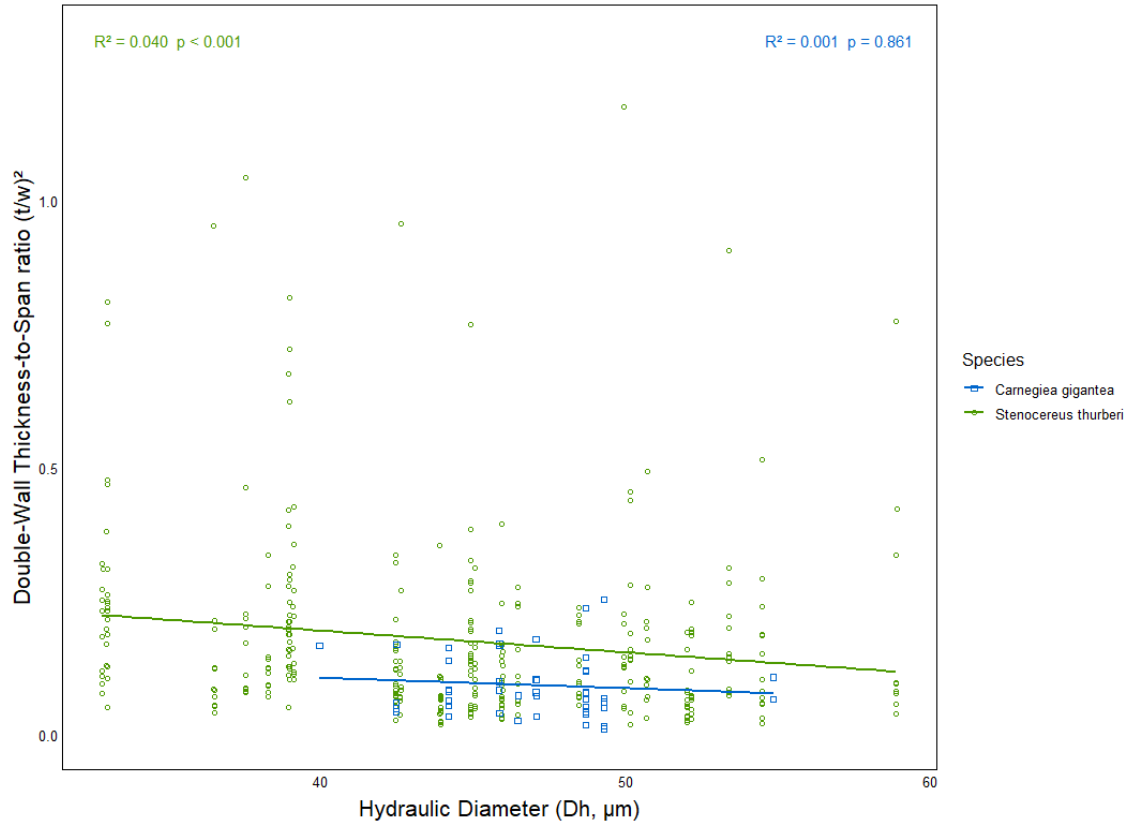


Figure 10. Double-wall thickness-to-span ratio $(t/w)_h^2$ over hydraulic diameter (D_h , μm) in *C. gigantea* ($b = -0.012$, $R^2 = 0.001$, $p = 0.861$) and *S. thurberi* ($b = -0.059$, $R^2 = 0.040$, $p < 0.001$).

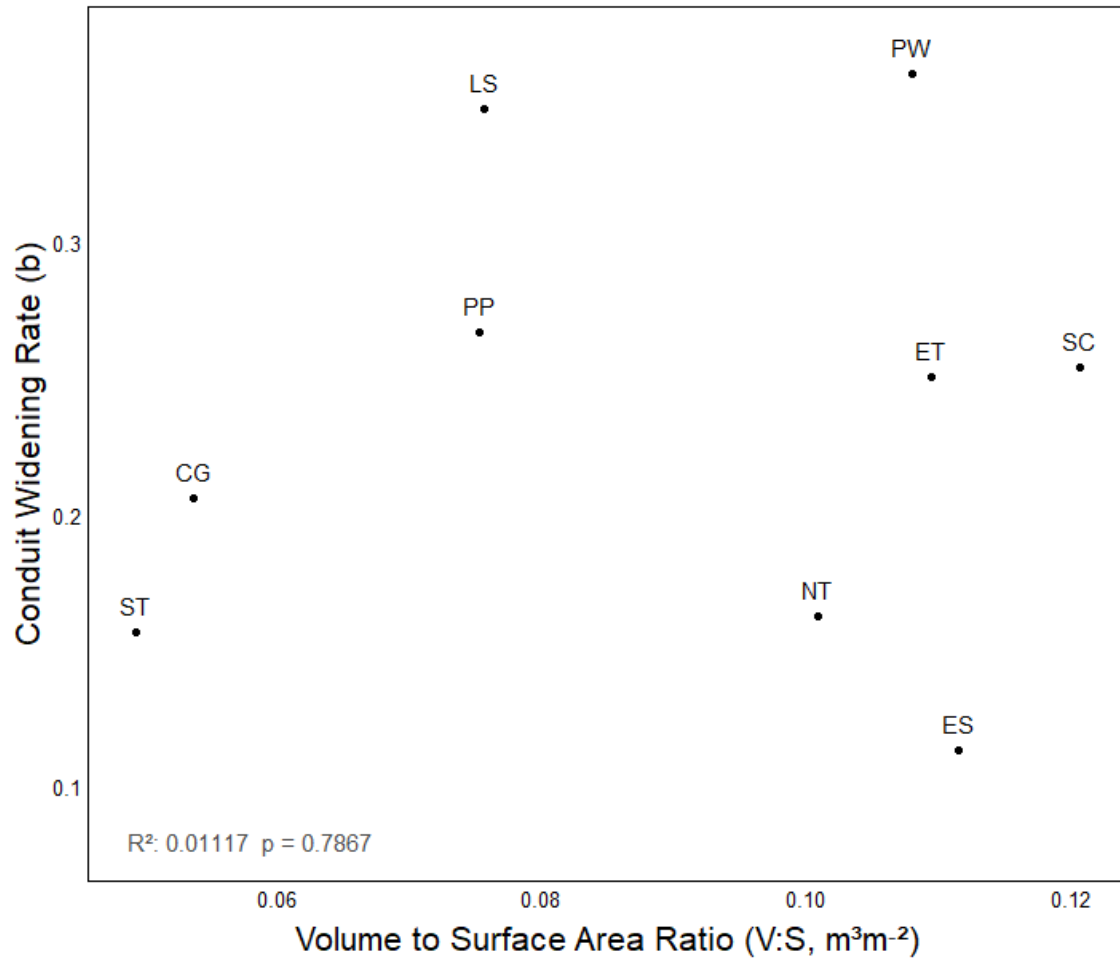


Figure 11. Conduit widening rates (b) of each species over their respective volume-to-surface-area ratio (V:S, m³m⁻²). No significant correlation ($R^2 = 0.011$, $p = 0.787$).

DISCUSSION

Cacti survive in arid conditions with limited rainfall by storing water in the cortex, the succulent parenchymatous tissue between the dermis layers and the inner ribs, and in the pith, the centermost tissue of the stem. The resulting reservoir of water decouples water transport into the stem from photosynthetic gas exchange and instead water transport is largely driven by osmotic gradients throughout the stem, making axial water transport independent from stomatal conductance. CAM photosynthesis is another factor of water use efficiency in cacti. By limiting carbon uptake to nighttime, and therefore keeping stomata closed during higher daytime temperatures, cacti are able to avoid excess water loss. Usage of CAM photosynthesis varies across different plant taxa, and cacti generally rely exclusively on this photosynthetic pathway (Berry *et al.*, 2013). Many species of giant cacti in North America—including *C. gigantea*, *Pachycereus pringlei*, *Lophocereus schottii*, and *S. thurberi*—surpass the water-use efficiency of other plants and appear to only express two of the four standard phases of the CAM cycle (Huber *et al.*, 2018; Hultine *et al.*, 2023). These unique water-use efficiency strategies allow cacti to thrive in arid environments while being under similar anatomical constraints as non-succulent woody taxa.

This study investigated several arborescent, multi-stemmed or columnar cacti (Cactaceae) species across multiple genera (Figure 11), and more specifically, the Cactoideae subfamily (Hernández-Hernández *et al.*, 2011). Within this clade, most of the genera in this study belong to Echinocereae, the second largest tribe of North American cacti (*Pachycereus*, *Neobuxbaumia*, *Carnegiea*, *Lophocereus*, *Stenocereus*); and Browningieae, a South American cactus tribe (*Stetsonia*) (Hernández-Hernández *et al.*,

2011; Guerrero *et al.*, 2018). *Echinopsis*, another South American genus, is generally polyphyletic (Hernández-Hernández *et al.*, 2011; Schlumpberger & Renner, 2012).

Within Echinocereeae, the genera can be further divided into two subtribes:

Pachycereinae (*Pachycereus*, *Neobuxbaumia*, *Carnegiea*, *Lophocereus*) and

Stenocereinae (*Stenocereus*) (Hernández-Hernández *et al.*, 2011; Guerrero *et al.*, 2018).

Across all species in this study, conduit diameters followed a significant basipetal widening rate of $b = 0.211$ (Figure 3A, $R^2 = 0.613$, $p < 0.001$), closely following universal scaling theory and conduit scaling measured in woody plant taxa ($b = 0.20$; Olson *et al.*, 2020; Soriano *et al.*, 2020). Xylem vessel density significantly decreased across all species along the length of the stem at an exponential rate of -0.701 (Figure 5, $R^2 = 0.715$, $p < 0.001$), and also had a similar significant inverse correlation with hydraulic mean diameter across all species (Figure 6, exponential rate: -2.804 , $R^2 = 0.751$, $p < 0.001$). Therefore, similar to non-succulent woody taxa, cactus stems balance out lower conductivity near the stem apex by having a greater density of vessels. As conduit vessels widen closer to the stem base, they are no longer present in such high density as smaller vessels are near the stem apex.

Columnar cacti across all genera display varying morphological and anatomical traits. For example, in *Stenocereus* and *Stetsonia*, the inner ribs fuse to form a wooden ring at the stem base while the plants are in early stages of development, whereas in *Carnegiea*, *Neobuxbaumia*, and *Pachycereus*, the ribs fuse only partially or not at all (Mozzi, 2021). Additionally, the stems of different species within Cactoideae display a range of volume-to-surface-area (V:S) ratios, which reflect physiological trade-offs between the water storage capacity of succulent tissues and whole-stem photosynthetic

capacity (Williams *et al.*, 2014; Hultine *et al.*, 2016). In species of *Stenocereus* and *Carnegiea*, for example, the former has a lower V:S ratio, and therefore has a greater capacity for growth under suitable conditions, while the latter has a greater capacity for water storage, which can be beneficial during times of drought (Hultine *et al.*, 2019).

Despite the various water use strategies of different columnar cactus species (Figure 10), the widening rates of each species were not significantly different from each other. Nonetheless, conduit widening rates ranged from 0.113 in *E. spachiana* to 0.361 in *P. weberi* (Figure 3B). In non-succulent woody taxa, conduit widening rates range from 0.1 to 0.3 within individuals (Olsen *et al.*, 2020). The species closest to universal scaling theory was *C. gigantea*, with a mean widening rate of 0.206; however, only three of six specimens had significant individual widening patterns. In both *S. thurberi* and *C. gigantea* there was also no significant difference between the individual specimens sampled ($n = 6$). Both *Pachycereus* species showed a higher widening rate than most other species (*P. weberi*: $b = 0.361$ and *P. pringlei*: $b = 0.267$). Other species with a widening rate above 0.20 included *Echinopsis terscheckii* ($b = 0.251$), *Stetsonia coryne* ($b = 0.254$), and *L. schottii* ($b = 0.349$). *E. spachiana*, *S. thurberi*, and *N. tetetzo* had widening rates below 0.20 ($b = 0.113$, $b = 0.157$, and $b = 0.163$, respectively). Figure 11 visualizes a phylogenetic tree for the nine species in this study and lists their respective rates of basipetal widening.

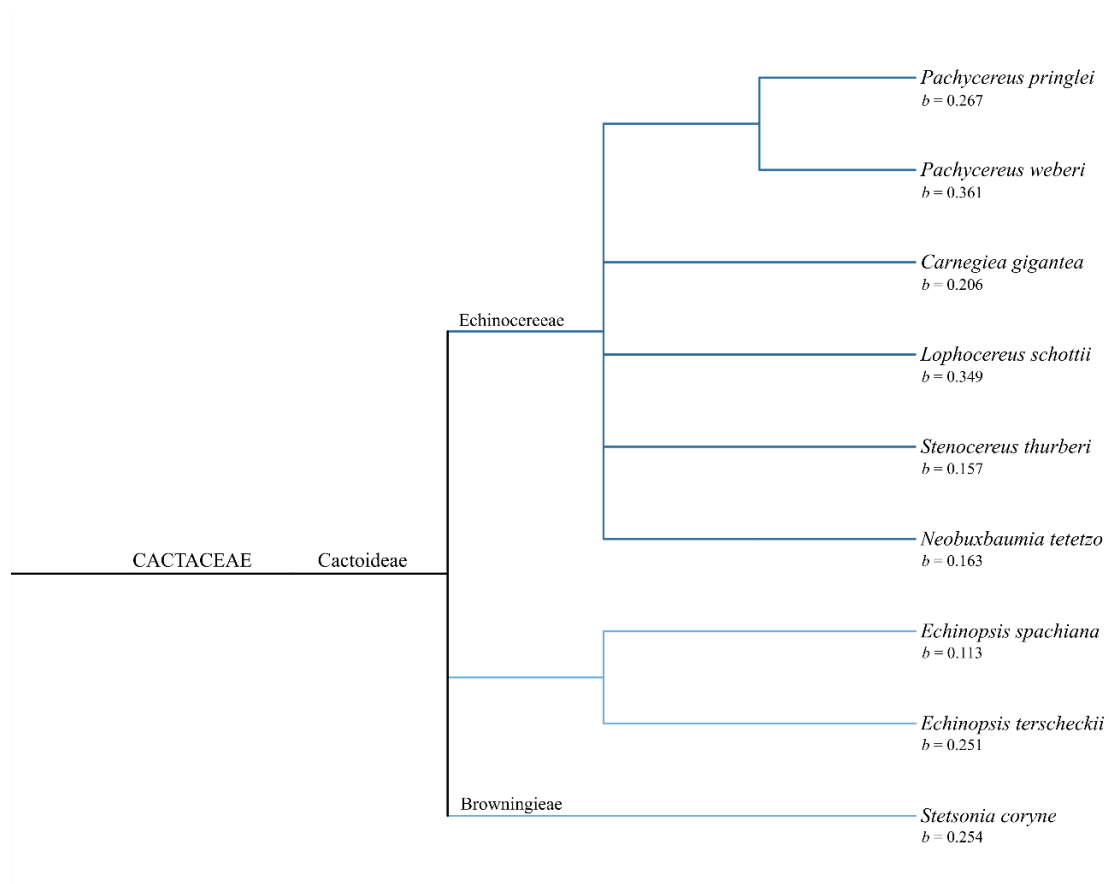


Figure 12. Phylogenetic tree of all nine columnar cactus species included in this study and their respective rate of basipetal widening, b . North American taxa are highlighted in dark blue and South American taxa are highlighted in light blue. Created using Interactive Tree of Life (iTOL version 6.7.1) and Cactaceae phylogenies from Hernández-Hernández *et al.* (2011) and Guerrero *et al.* (2018).

Exponentially decreasing vessel density along the length from the stem apex was also not significant between individual species, although there was a range of exponential rates of change from -1.174 in *N. tetetzo* to -0.358 in *E. spachiana* (Figure 7). Among the species with higher exponential rates of decreasing vessel density, those of *N. tetetzo* and *P. schottii* were -1.174 and -1.035, respectively. The lowest exponential rate belonged to *E. spachiana* (-0.358), while the next lowest belonged to *E. terscheckii* (-0.625). The rest of the species had more modest exponential rates above -0.701, the mean exponential rate of vessel density decrease across all species sampled. Similar to conduit widening comparisons between individual specimens sampled, there was also no significant difference in vessel density exponential rates of decrease between the individual stems in both *C. gigantea* and *S. thurberi*.

Double-wall thickness-to-span ratio illustrates the relative structural stability of xylem conduit bundles. When the ratio of double-wall thickness to span is higher, paired conduit vessels are less likely to embolize and implode due to greater reinforcement of the shared conduit wall (Hacke *et al.*, 2001). Double-wall thickness-to-span ratio in *C. gigantea* did not show significant correlation to either the length from the stem apex or hydraulic diameter (Figure 8: $R^2 = 0.012$, $p = 0.467$; Figure 9: $R^2 = 0.001$, $p = 0.861$). In *S. thurberi*, there was a significant but weak correlation to both the length from the stem apex and hydraulic diameter, with very low rates of decrease (Figure 8: $R^2 = 0.024$, $p = 0.005$; Figure 9: $R^2 = 0.040$, $p < 0.001$). Therefore, both the threat and resistance to cavitation in paired xylem conduits throughout the length of the stem show no particular trend. In other words, despite observing larger-sized conduits near the stem base, there is

little to no increased chance of spreading embolism through xylem conduits along the length of the stem.

Not only was there no significant difference in hydraulic architectural trait patterns between phylogenetically diverse species with various stem morphologies, but there was also no significant correlation between conduit widening rates and volume-to-surface-area ratios (Figure 10). Therefore, stem succulence and water storage behavior in cacti may be separate from internal hydraulic architecture. If conduit widening is also an adaptation in cacti, as it is non-succulent woody taxa (Olson *et al.*, 2020), then perhaps succulence in cacti developed at a later stage of evolution and the unique water-use efficiency strategies of cacti are the key to thriving in arid environments despite being under similar anatomical constraints as woody taxa. Cacti are of great ecological importance in arid ecosystems, yet they are also among the most threatened and endangered taxa on the planet (Hultine *et al.*, 2023). Understanding how cacti cope with severe water limitations is crucial to desert ecology, especially with changing climates and rising temperatures.

CONCLUSION

This study demonstrates that cactus xylem anatomy does not deviate from universal scaling theory, regardless of the water storage and water use behavior unique from woody plant taxa: rather than by stomatal regulation, the primary driver of long-distance water transport in succulent-stemmed plants such as cacti are osmotic gradients in storage tissues. Xylem conduit widening closely follows the universal widening pattern of woody tree species and xylem vessel density trends compensate for changes in xylem conduit size to maintain hydraulic conductivity throughout the stem. Both conduit widening rates and vessel density do not significantly vary between phylogenetically diverse columnar cactus species despite their various water storage behaviors and stem morphologies. Double-wall thickness-to-span ratio lacks strong correlation with either length or hydraulic diameter; in other words, the threat of spreading embolism through bundles of bordering xylem conduits may remain constant regardless of anatomical differences along the stem. Across phylogenetically and morphologically diverse species of giant cacti, we find similar anatomical patterns that do not significantly deviate from each other. Additionally, we found no significant correlation between conduit widening patterns and water-use behaviors, represented by the diverse volume-to-surface-area ratios of each columnar cactus species. Thus, stem succulence and water storage behavior in cacti may be separate from internal hydraulic architecture.

Giant cacti follow similar internal anatomical constraints as non-succulent woody taxa, and rather than occurring despite the unique water use behaviors and adaptations in cacti, it is due to these adaptations that they are able to thrive in arid environments while being under similar constraints as other vascular plants. Investigating xylem architecture

in cacti helps us understand how these species cope with severe water limitations and provides new insights on evolutionary constraints of stem succulents as they functionally diverged from other life forms.

REFERENCES

- Anfodillo, T., Carraro, V., Carrer, M., Fior, C., Rossi, S. (2006). Convergent tapering of xylem conduits in different woody species. *New Phytologist*, 169, 279-290. <https://doi.org/10.1111/j.1469-8137.2005.01587.x>
- Anfodillo, T., Petit, G., & Crivellaro, A. (2013). Axial conduit widening in woody species: a still neglected anatomical pattern, *IAWA Journal*, 34(4), 352-364. <https://doi.org/10.1163/22941932-00000030>
- Berry, J.O., Yerramsetty, P., Zielinski, A.M. *et al.* (2013). Photosynthetic gene expression in higher plants. *Photosynthesis Research*, 117, 91–120. <https://doi.org/10.1007/s11120-013-9880-8>
- Caspeta, I. (2022). Water relations of giant cacti of the Sonoran Desert. Arizona State University: Barrett, The Honors College. KEEP. <https://hdl.handle.net/2286/R.2.N.168230>
- Bräutigam, A., Schlüter, U., Eisenhut, M., Gowik, U. (2017). On the Evolutionary Origin of CAM Photosynthesis. *Plant Physiology*, 174(2), 473-477. <https://doi.org/10.1104/pp.17.00195>
- Fichot, R., Barigah, T.S., Chamaillard, S., Le Thiec, D., Laurans, F., Cochard, H. And Brignolas, F. (2010). Common trade-offs between xylem resistance to cavitation and other physiological traits do not hold among unrelated *Populus deltoides* × *Populus nigra* hybrids. *Plant, Cell & Environment*, 33, 1553-1568. <https://doi.org/10.1111/j.1365-3040.2010.02164.x>
- Hacke, U., Sperry, J., Pockman, W. *et al.* (2001). Trends in wood density and structure are linked to prevention of xylem implosion by negative pressure. *Oecologia*, 126, 457–461. <https://doi.org/10.1007/s004420100628>
- Hernández-Hernández, T., Hernández, H.M., De-Nova, J.A., Puente, R., Eguiarte, L.E. and Magallón, S. (2011). Phylogenetic relationships and evolution of growth form in Cactaceae (Caryophyllales, Eudicotyledoneae). *American Journal of Botany*, 98, 44-61. <https://doi.org/10.3732/ajb.1000129>
- Hultine, K.R., Williams, D.G., Dettman, D.L. Butterfield, B. J., Puente-Martinez, R. (2016). Stable isotope physiology of stem succulents across a broad range of volume-to-surface area ratio. *Oecologia*, 182, 679–690. <https://doi.org/10.1007/s00442-016-3690-6>

- Hultine, K. R., Dettman, D. L., English, N. B., Williams D. G. (2019). Giant cacti: isotopic recorders of climate variation in warm deserts of the Americas. *Journal of Experimental Botany*, 70(22), 6509-6519. <https://doi.org/10.1093/jxb/erz320>
- Hultine, K. R., Hernández-Hernández, T., Williams, D. G., Albeke, S. E., Tran, N., Puente, R., Larios, E. (2023). Global change impacts on cacti (Cactaceae): current threats, challenges and conservation solutions. *Annals of Botany*, XX, 1-13. <https://doi.org/10.1093/aob/mcad040>
- Mauseth, J. D. (2000). Theoretical aspects of surface-area-to-volume ratios and water-storage capacities of succulent shoots. *American Journal of Botany*, 87(8), 1107–1115. <https://doi.org/10.2307/2656647>
- Mauseth, J. D. (2006). Structure-function relationships in highly modified shoots of Cactaceae. *Annals of Botany*, 98, 901-926. <https://doi.org/10.1093/aob/mcl133>
- McCulloh, K.A., Sperry, J.S., Adler, F.R. (2003). Water transport in plants obeys Murray's law. *Nature*, 421(6926), 939-42. <https://doi.org/10.1038/nature01444>
- Mozzi, G., Romero, E., Martínez-Quezada, D. M., Hultine, K., Crivellaro, A. (2021). PEG infiltration: an alternative method to obtain thin sections of cacti tissues. *IAWA Journal*, 42(2), 204-208. <https://doi.org/10.1163/22941932-bja10051>
- Mozzi, G. (2021). Succulent plants: insight on the adaptive strategies to extreme environments. [Unpublished PhD thesis]. University of Padova.
- Nobel, P.S. (1991). Achievable productivities of certain CAM plants: basis for high values compared with C3 and C4 plants. *New Phytologist*, 119, 183-205. <https://doi.org/10.1111/j.1469-8137.1991.tb01022.x>
- Nobel, P.S. (1996). Responses of some North American CAM plants to freezing temperatures and doubled CO2 concentrations: implications of global climate change for extending cultivation, *Journal of Arid Environments*, 34(2), 187-196. <https://doi.org/10.1006/jare.1996.0100>.
- Olson, M. E., Anfodillo, T., Rosell, J. A., Petit, G., Crivellaro, A., Isnard, S., Leon-Gomez, C., Alvarado-Cardenas, L. O., Castorena, M. (2014). Universal hydraulics of the flowering plants: vessel diameter scales with stem length across angiosperm lineages, habits and climates. *Ecology Letters*, 17, 988-997. <https://doi.org/10.1111/ele.12302>
- Olson, M. E., Anfodillo, T., Gleason, S. M., McCulloh, K. A. (2020). Tip-to-base xylem conduit widening as an adaptation: causes, consequences, and empirical priorities. *New Phytologist*, 229, 1877-1893. <https://doi.org/10.1111/nph.16961>

- Posit team (2022). RStudio: Integrated Development Environment for R. Posit Software, PBC, Boston, MA. URL <http://www.posit.co/>.
- R Core Team (2022). R: A language and environment for statistical computing. R Foundation for Statistical Computing, Vienna, Austria. URL <https://www.R-project.org/>.
- Schlumpberger, B.O. and Renner, S.S. (2012). Molecular phylogenetics of *Echinopsis* (Cactaceae): Polyphyly at all levels and convergent evolution of pollination modes and growth forms. *American Journal of Botany*, 99, 1335-1349. <https://doi.org/10.3732/ajb.1100288>
- Schneider, C. A., Rasband, W. S., & Eliceiri, K. W. (2012). NIH Image to ImageJ: 25 years of image analysis. *Nature Methods*, 9(7), 671–675. <https://doi.org/10.1038/nmeth.2089>
- Silvera K., Neubig K. M., Whitten W. M., Williams N. H., Winter K., Cushman J. C. (2010). Evolution along the crassulacean acid metabolism continuum. *Functional Plant Biology*. 37, 995-1010. <https://doi.org/10.1071/FP10084>
- Soriano, D., Echeverría, A., Anfodillo, T., Rosell, J. A., Olsen, M. E. (2020). Hydraulic traits vary as the result of tip to base conduit widening in vascular plants. *Journal of Experimental Botany*, 71(14), 4232-4242. <https://doi.org/10.1093/jxb/eraa157>
- Sperry, J.S. and Tyree, M.T. (1988). Mechanism of water stress-induced xylem embolism. *Plant Physiology*, 88, 581-587. <https://doi.org/10.1104/pp.88.3.581>
- Sperry, J.S., Nichols, K.L., Sullivan, J.E.M. and Eastlack, S.E. (1994). Xylem embolism in ring-porous, diffuse-porous, and coniferous trees of northern Utah and interior Alaska. *Ecology*, 75, 1736-1752. <https://doi.org/10.2307/1939633>
- West, G.B., Brown, J.H., Enquist, B.J. (1999). A general model for the structure and allometry of plant vascular systems. *Nature*, 400, 664– 667. <https://doi.org/10.1038/23251>
- Wickham, H., Averick, M., Bryan, J., Chang, W., McGowan, L. D., François, R., Grolemund, G., Hayes, A., Henry, L., Hester, J., Kuhn, M., Pedersen, T. L., Miller, E., Bache, S. M., Müller, K., Ooms, J., Robinson, D., Seidel, D. P., Spinu, V., Takahashi, K., Vaughan, D., Wilke, C., Woo, K., Yutani, H. (2019). Welcome to the tidyverse. *Journal of Open Source Software*, 4 (43), 1686. <https://doi.org/10.21105/joss.01686>
- Williams, D. G., Hultine K. R., and Dettman, D. L. (2014). Functional trade-offs in succulent stems predict responses to climate change in columnar cacti. *Journal of Experimental Botany*, 65(13), 34053413. <https://doi.org/10.1093/jxb/eru174>

Winter, K., Aranda, J., and Holtum, J. A. M. (2005). Carbon isotope composition and water-use efficiency in plants with crassulacean acid metabolism. *Functional Plant Biology*, 32, 381-388. <https://doi.org/10.1071/FP04123>